LATVIAN JOURNAL OF PHYSICS AND TECHNICAL SCIENCES
2008, N 4

10.2478/v10047-008-0019-1

NEUTRON LAUE DIFFRACTION IN PERFECT AND DEFORMED SILICON SINGLE CRYSTALS UNDER ULTRASOUND EXCITATION

E. Raitman, V. Gavrilov and M. Brezgunov

Institute of Physical Energetics,
21 Aizkraukles Str., Riga, LV-1006, LATVIA

The effect of ultrasound (US) on neutron Laue's diffraction is studied for perfect and deformed crystals. In a perfect crystal the oscillations of relative diffraction intensity were observed, which depend on the ultrasound wave amplitude. In a deformed crystal the ultrasound distorts the adiabatic motion of the image points along the sheets of dispersive surface. This gives rise to the diffraction intensity behavior which sharply differs from that in the perfect crystal case. The results obtained agree well with theoretical concepts. The described effects can be used for creation of US-controlled new type neutron monochromators or choppers.

1. INTRODUCTION

The influence of ultrasound (US) waves on the neutron and X-ray scattering is described in a number of works [1–8]. In contrast to X-ray diffraction, when the X-ray – acoustic resonance is determined by the condition $\lambda_s = \tau$ (λ_s being the US wave length and τ the extinction length), in the case of neutrons the main role in the scattering is played by the Doppler effect or the energy exchange between neutron and acoustic phonons. Depending on the parameters of US wave such as its amplitude, length, and frequency as well as on the length of radiation extinction in a crystal, the different scattering modes could be distinguished: a) if frequency of ultrasound ν_s is lower than that of neutron-acoustic resonance ν_{res}, US effect can be considered as a diffraction on smooth and time-dependent lattice deformations; b) if $\nu_s >> \nu_{res}$ the US mixes the states corresponding to different sheets of the dispersion surfaces, producing self-intersection points and a new area of the total reflection governed by US. This leads to a new type of oscillations depending on the acoustic wave amplitudes [9]. These oscillations become more contrast at approaching the conditions of neutron acoustic resonance.

In deformed crystals, which are of great practical interest, the effect of US on diffraction has been investigated much less. In [10], the results of theoretical and experimental investigations of neutrons and X-rays for the case of Laue diffraction in deformed silicon single crystals under high-frequency ($\nu_s >> \nu_{res}$) excitation are reported. The analysis has shown that in a smoothly deformed Si crystal ultrasound results in violation of the adiabatic conditions for the movement of tie points on the dispersion surfaces. Owing to this, a drastic decrease in the diffraction intensities was observed for low acoustic wave amplitudes. With the amplitudes increasing the intensity also increases, reaching the kinematical limit. In absolute values, the influence of the US is much stronger manifested in the diffraction on a deformed crystal than on an ideal one. A substantial role is played by multiphonon processes. The presence of static strains leads to the appearance of a new type of oscillations, which depend on the deformation gradient.

This work is aiming at studying experimentally the interference beats (the so-called pendellősung) of a diffracted neutron beam in perfect and low-deformed silicon monocrystals under various conditions of US excitation.

2. EXPERIMENTAL

Figure 1 shows a scheme of diffraction measurements in the Laue geometry. The neutrons with a wavelength of 1 Å after monochromator (1) are collimated by Soller's collimator (2) and controlling diaphragm (3) which form a beam with divergence not worse than 5'.

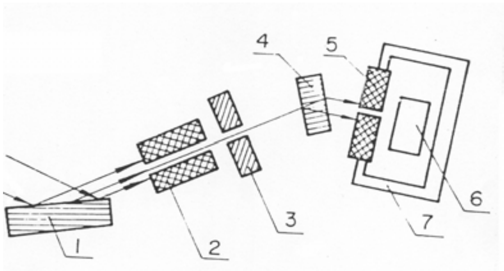

Fig. 1. Scheme of diffraction measurements:
1 – crystal-monochromator; *2* – collimator; *3* – controlling diaphragm;
4 – sample; *5* – analysing slit; *6* – detector; *7* – scanning device.

As the sample, a dislocation-free silicon single crystal with a thickness of 1.73 mm and a diameter of 76 mm was used. In such a Laue-symmetrical geometry the intensity of (220) reflections was measured using a simple one-crystal diffractometer. The neutron wavelength was 0.1 nm with monochromatisation not worse than 1%. The beam's collimation was not worse than 5', making it possible to scan the diffracted radiation from different parts of the single crystal with the purpose to choose a section with uniform spatial distribution of the acoustic field.

The sample was bent using an ordinary so-called four-point bending device [12]. The device allowed the sample to be turned with respect to vector **H** of the reciprocal lattice by angle φ without changing the set diffraction angle Θ_B. In this case, apart from the change in the effective crystal thickness, the diffraction intensity is defined by the projection of the deformation gradient $|\mathbf{B}_{pr}|$ onto the scattering plane – i.e. by the slope φ, although the deformation gradient **B** (bending) was set arbitrarily and remained unchanged. The scanning device (7) allowed measuring the spatial distribution of the scattered neutrons or the acoustic field uniformity in the sample. The width of the analysing slit could be varied in the range 0.3–2.0 mm.

A transverse US wave ($\mathbf{K_s} \perp \mathbf{K_0}$, **H**; $\mathbf{W} \| \mathbf{H}$, where $\mathbf{K_s}$ and $\mathbf{K_0}$ are the wave vectors for sound and neutrons, **W** is the amplitude of ultrasound wave) was excited in a crystal with a quartz piezotransducer grinded to the sample by epoxy resin without hardener. The first harmonic ν_s = 14.84 MHz close to the main frequency of piezotransducer (15 MHz) was used to make possible the operation near the neutron acoustic resonance frequency ν_{res} = 14.71 MHz. In Fig. 2 the normalized diffraction intensity is shown in dependence on angle φ (B_{pr}).

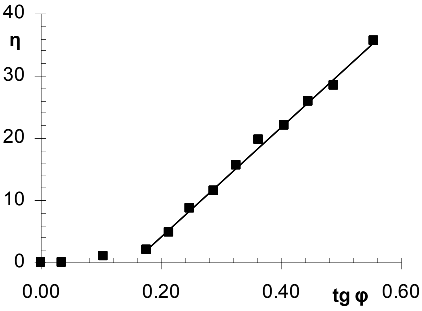

Fig. 2. Relative changes of the diffraction intensities $\eta = (I_d - I_0)/I_0$ in a deformed crystal for (220) reflection depending on slope φ. Sound is switched off. The solid straight line is consistent with the theory [13].

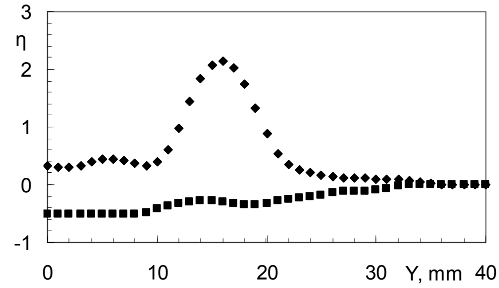

Fig. 3. Distribution of the relative diffraction intensities for perfect (♦) and deformed (■) crystals $\eta = (I_s - I_0)/I_0$ and $\eta = (I_{ds} - I_{d0})/I_{d0}$, where subscripts 0, *d* denote perfect (without sound) and deformed crystal, respectively, and *s* – when US is switched on. US frequency ν_s = 14.84 MHz, analysing slit width 1 mm.

This dependence can be used for determination of the B_{pr} value. As was shown earlier [14], to observe the interference effects associated with the neutron scattering from the ultrasound lattice oscillations a good uniformity of the acoustic field inside the crystal is needed: $\Delta W/W$ not worse than 10%. Figure 3 shows the US influence on the relative intensity of the neutron diffraction in a perfect and a deformed crystal. The results of scanning along the sample diameter – apart from demonstration of evident differences between such crystals – allow a crystal section to be chosen that would have a uniform acoustic field distribution: $Y = 15\pm1$ mm, where $\Delta W/W$ is not worse than 5%.

Figure 4*a,b,c* displays the frequency dependence of diffraction intensities and the fine structure of these intensities *vs.* frequency. The measurements were performed with small steps; the data show that standing waves are created in the crystal. This subject is developed below in the discussion. Note that the distance between the main peak and the frequency satellites does not depend on the resonance harmonic excited in the crystal or on the presence of weak deformations.

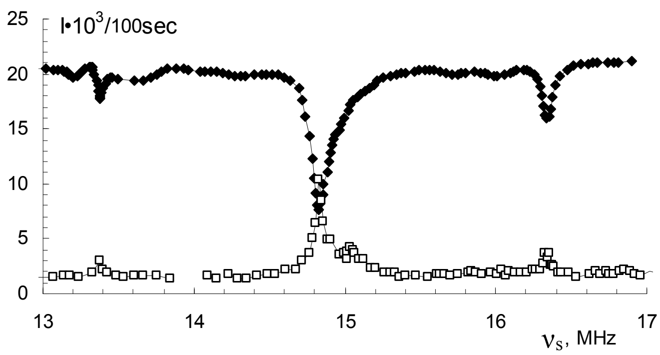

Fig.4a. Diffraction intensity *vs.* ultrasound frequency. The lower curve relates to the perfect crystal (□)and the upper curve (◆) to the deformed one.

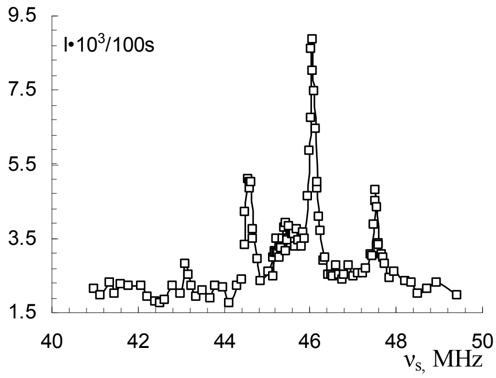

Fig. 4b. The same as in Fig.4*a* for the perfect crystal and third harmonic.

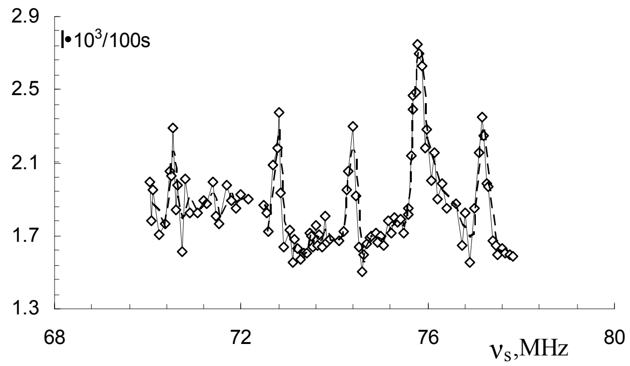

Fig.4c. The same as in Fig.4*a,b* for the perfect crystal and fifth harmonic.

3. THEORETICAL BACKGROUND

Figure 5 presents a schematic view of the dispersion surface (DS) changes for perfect and deformed crystals under the US influence.

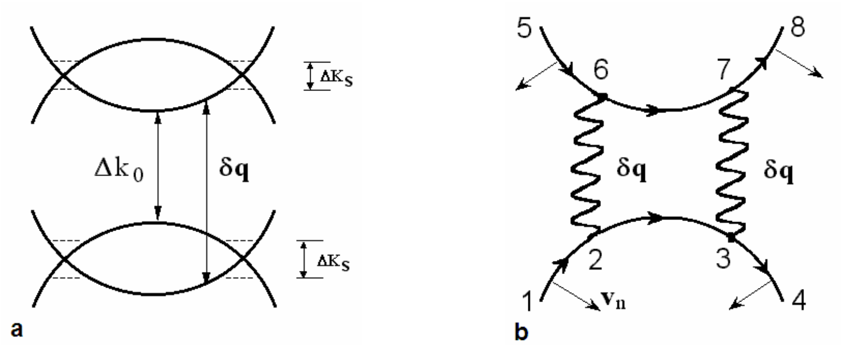

Fig. 5. Dispersion surfaces of a crystal modified by ultrasound: *a*) dispersion surface of a neutron in the perfect crystal for transversal acoustic waves; *b*) dynamics of travelling of tie points in a deformed crystal.

In the case of perfect crystal, as shown in Fig. 5*a*, a DS shift by δq occurs, which is

$$\delta q = 2\pi f_s / v_n \cos \Theta_B \pm k_s \tag{1}$$

and the resonance frequency is then

$$v_{res} = \frac{v_s}{\tau}\left|\cos\varphi \pm \frac{v_s}{v_n\cos\Theta_B}\right|^{-1}. \tag{2}$$

At the intersection points the ultrasound takes off the degeneration of the pulse state, and on the DS additional slits arise:

$$\Delta K_S = (\mathbf{HW})\,\Delta k_0\,, \tag{3}$$

which determine the appearance of the diffraction intensity oscillations at low US wave amplitudes.

The theoretical basis of interaction between neutron and acoustic phonons is outlined in [9], where various situations are considered from the viewpoint of the relationship between the extinction length, τ, and the acoustic wave length, λ_s.

The mentioned work considers the Laue-symmetrical diffraction of neutrons in a two-wave approximation when the propagation of neutron waves in a crystal with static or dynamic (US) deformations is described by the Takagi–Taupin equations:

$$i\frac{\partial\Psi_0}{\partial s_0} + \exp(i\,\mathbf{HW})\frac{\Delta k_0}{2}\cos\Theta_B\Psi_h = 0\,,$$
$$i\frac{\partial\Psi_h}{\partial s_h} + exp(i\,\mathrm{HW})\frac{\Delta k_h}{2}cos\,\Theta_B\Psi_0 = 0\,, \tag{4}$$

where Ψ_0, Ψ_h, and k_0, k_h are the amplitudes and wave vectors of the incident and diffracted radiation beams; s_0, s_h are the coordinates along the k_0, k_h vectors; The displacement of nuclei, U, is introduced in form (5), where a, b, and c are numerical constants describing inhomogeneous deformation; $\mathbf{U}_s$ is the nuclear displacement in the acoustic field, and $\mathbf{U}_d$ is the static displacement associated with the lattice deformation:

$$\mathbf{HU} = \mathbf{HU}_s + \mathbf{HU}_d\,;$$
$$\mathbf{HU}_s = 4\mathbf{HW}\cos[k_s(s_0+s_h)\cos\Theta_B]\cos(\omega_s t)\,;$$
$$\mathbf{HU}_d = 2as_0^2 + 4bs_0s_h + 2cs_h^2\,;$$
$$B = b[2/(\Delta k_0\cos\Theta_B)]^2\,;\qquad C = c[2/(\Delta k_0\cos\Theta_B)]^2\,. \tag{5}$$

In the quasi-classical approximation (B <<1 but BT >>1, where B is the gradient of deformation), for **HW** < 1, assuming that $k_s/\Delta k_0 = \alpha$ we will have analytical expressions (6a, 6b, 6c) for relative intensity variations depending on the relationship between k_s and k_0. If the frequency of acoustic waves is higher than the resonance frequency (v_{res}, $\alpha > 1$) the second term in (6c) describes the so-called deformative oscillations whose period depends on B and $\tilde{\alpha}$.

$$\eta = 1 - \frac{I_h(\mathbf{HW},B)}{I(0,0)} = \frac{\pi[HW\cos(\omega t)]^2}{B[8(1-\alpha)]^{1/2}}\times\exp\left(-\frac{2^{5/2}(1-\alpha)^{3/2}}{3B}\right),\qquad \alpha<1 \tag{6a}$$

$$\eta = \frac{\left(\mathbf{HW}\cos(\omega t)\Gamma(1/3)\right)^2}{2(6^{1/3})B^{4/3}}, \qquad \alpha \approx 1 \quad (6b)$$

$$\eta = \frac{\pi[\mathbf{HW}\cos(\omega t)]^2\alpha}{B(\alpha^2-1)^{1/2}} \times \left[1+\sin\left(\frac{(\alpha^2-1)\alpha}{2B} + \operatorname{arcsin} h(\alpha^2-1)^{1/2}\right)\right], \quad \alpha > 1 \quad (6c)$$

The experimental verification of the validity of expressions (6a-c) is one of the main tasks of the work presented.

4. RESULTS AND DISCUSSION

4.1. Standing acoustic waves

The presence of satellites shown in Fig. 4*a–c*, which exist at equal distance from the main peak in the perfect and slightly deformed crystals independently of the chosen frequency interval, is the evidence for excitation of standing waves in the crystal.

For standing waves the relation $T = n\,\lambda_s/2$ (where n is the whole number of US half-waves, λ_s is the US wavelength and T is the distance travelled by US waves) will be valid. Knowing T and the distance between the maxima (minima) $\Delta\nu_s = \nu_{sn} - \nu_{s(n\pm1)}$, the number of mechanical self-resonance harmonics n and the sound velocity v_s in the [111] direction parallel to the scattering plane can be determined. Defining $\Delta\nu_s$ from the dependences shown in Fig. 4*a–c*, where $\Delta\nu_s =$ = (1.475. ± 0.046) MHz one can see that the number of transverse half-waves is $n =$ = 10 for ν_s= 14.836 MHz and $v_{s[111]} = 5.13\ 10^5$ cm/s. This value is very close to the reference data of 5.09 10^5 cm/s (see [15]).This means that the values of US wave velocities in crystals can be determined with neutron and X-ray diffraction technique, and that this method is applicable for, e.g., determination of the sound velocity at phase transitions.

4.2. Perfect crystal. Oscillations depending on the US wave amplitude

Figure 6 clearly shows at least four oscillations associated with appearance of new areas of total reflection. The experimental data agree with the results of the numerical calculations based on Takagi–Taupin's equations (Eqs. (4)) for $B = 0$ in

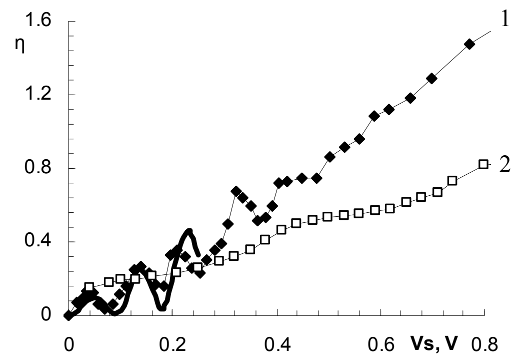

Fig. 6. Relative diffraction intensity variation for perfect crystal *vs*. generator voltage: *1*) US frequency ν_s = 14.84 MHz ($\alpha \approx 1$).; *2*) the same as curve 1 but for ν_s = 46.04 MHz ($\alpha \approx 3$). The fitting shown as a solid curve is obtained from numerical calculations (Eq. (4)).

the one-phonon approximation. The calculations were performed using the relationship **HW** = cV_S. The best coincidence of calculations with the experiment is at $c = 0.14$. The frequency of measurements was 14.84 MHz, which is very close to the calculated frequency of the neutron-acoustic resonance equal to 14.71 MHz. The contrast of the oscillations $\rho = (\eta_{\max} - \eta_{\min})/(\eta_{\max} + \eta_{\min})$ is (17.5 ± 4.6)%. For a frequency much higher than resonant (curve *2* of Fig. 6) traces of oscillations with a negligibly low contrast could only be observed; this result coincides qualitatively with theoretical predictions [9].

Therefore the experimental data confirm the validity of the theoretical predictions. The oscillating dependences $\eta = f(V_s)$ could be used for determination of very low amplitudes of US waves.

4.3. A deformed crystal. Oscillations depending on the deformation gradient

For the Laue diffraction in uniformly deformed crystals the problem was analysed in [10]. As distinguished from the perfect crystal case where for the whole crystal a unitary dispersion surface exists, in the Penning–Polder–Kato model [13] to each point of a bent crystal an own two-sheet dispersive surface corresponds, and the neutron is travelling adiabatically inside the crystal without transitions of the excited tie point between the DS sheets. The role of ultrasound in this model consists in the resonant suppression of adiabatic movement of the tie points. The one-phonon absorption corresponds to path 1–2–6–7–8 of the tie point along the dispersion surface (Fig. 5*b*). The neutron incident on the crystal excites points 1 and 8 on the DS. In the absence of ultrasound, point 1 travels along path 1–2–3–4 and passes into the state corresponding to a diffracted wave. Point 8 makes no contribution to the diffraction. When US is switched on, the movement of point 8 is not disturbed. As concerns point 1, it can reach state 4 by two ways: a) 1–2–6–7–3–4 or b) 1–2–3–4. If the probability for the excitation point to remain on DS sheets at points 2, 3 6, and 7 is P, and the probability to pass onto another DS sheet owing to the US disturbance is M ($P+M = 1$), then the probability of the former process is equal to M^2, the probability of the latter process is equal to P^2, and the change in the relative diffraction intensity will be

$$\eta = (I_{ds} - I_{d0}) / I_{d0} = P^2 + M^2 - 1 = -2MP < 0\,. \tag{7}$$

The probability of transition for the excitation point in the case of Laue's diffraction is approximately described as

$$M \approx 1 - \exp[-\pi (Hw)^2 / 2B], \tag{8}$$

where B is the deformation gradient determined from the expression:

$$I_d/I_0 - 1 = 4(BT/\tau)\,\mathrm{tg}\varphi \tag{9}$$

and from Fig. 2, which takes into account the change in the effective crystal thickness $T_{eff} = T/\cos\varphi$.

The maximum transition probability is 0.5, and, correspondingly, $\eta_{\max} = 0.5$ according to expression (7). However, the interference effects associated with two different paths travelled by the neutron inside the crystal in the presence of ultrasound excitation, being averaged, are not accounted for in expressions (7) and (8) but are described by expression (6c). Figure 7 shows relative intensity variations (I_{ds}/I_{d0}) for $\alpha = 3.13$ depending on the US wave amplitude.

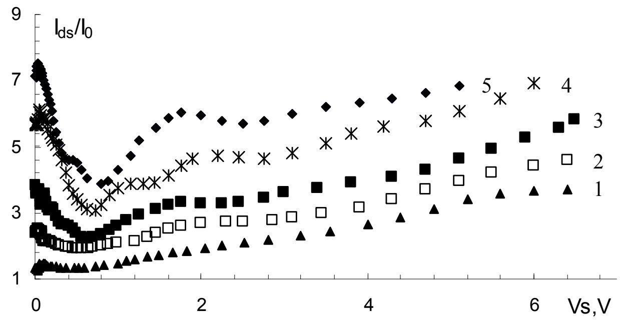

Fig. 7. Variations in the relative intensity of diffraction in a deformed crystal *vs.* voltage on piezotransducer for α =3.13 (v_s = 46.04 MHz) and different B: *1* – 0.023(▲); *2* – 0.052 (□); *3* – 0.083 (■); *4* – 0.124 (✻); *5* –0.166 (♦); I_0 is the diffraction intensity in a perfect crystal without sound; I_{ds} the same for a deformed one.

Figure 8 displays the variations in the diffraction intensity in the case of $\alpha \approx 1$ for a deformed crystal depending on the voltage on the piezotransducer and on the deformation gradient. Apart from a noticeable shift of the minimum position with B increasing towards higher voltages it could be seen that the maximum value of the relative changes of I_{ds} at $\alpha = 1$ (the neutron-acoustic resonance) is 0.7, which means that the probability of US-induced transitions of the tie point from one sheet of the dispersive surface to another is in this case higher than for $\alpha = 3.13$.

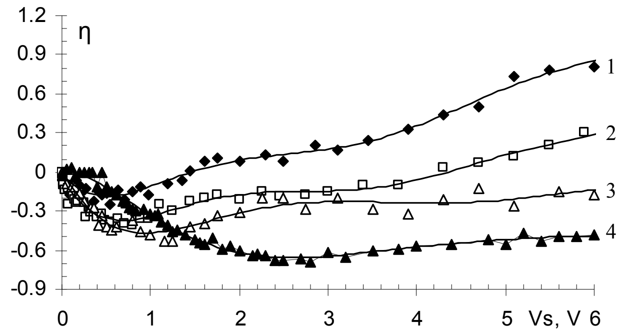

Fig. 8. Relative diffraction intensity *vs.* piezotransducer voltage for different values of parameter B: *1*) – 0.06, *2*) – 0.11, *3*) –0.23, *4*) –0.89; v_s=14.84 MHz ($\alpha \approx 1$). The best fitting is obtained using series expansion of the Bessel functions $J_0\left[\frac{(\mathbf{HW})^2}{B^{4/3}}\right]$ (solid curves).

The straight (2) and dashed (1) lines in Fig. 9 were obtained by the least squares method. The best fitting is at $|\eta_{\min}| = 0.55{\cdot}(1/B)^{-0.99}$ ($R^2 = 0.87$) for curve (*1*) and $|\eta_{\min}| = -0.04B^1+0.74$ ($R^2 = 0.98$) for curve (*2*) where R^2 is a reliability coefficient. From there it follows that at $B \sim 1$ the “dip” of the relative diffraction intensity η reaches the maximum of ~0.5 for $v_s >> v_{res}$ and of 0.7 for $v_s \approx v_{res}$. The strong effect near the neutron-acoustic resonance, by analogy with the resonance destruction of Bormann's effect [11] (the X-ray – acoustic resonance) can be qualitatively explained by the fact that the transitions between DS branches in the case of their contact occur in a much greater volume of the pulse space.

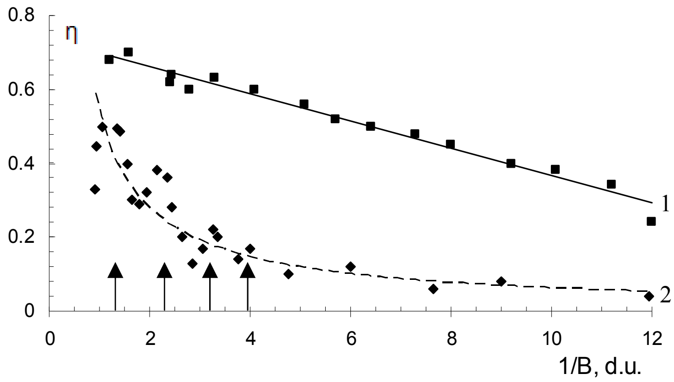

Fig. 9. The module of "dip" maximum depth $\eta = |I_{ds}\text{-}I_{d0}|/I_{d0}$ *vs*. the inverse value of the deformation gradient B (in dimensionless units according to Eq. (9)): *1* – for $\nu_s = 14.84$ MHz (near to neutron acoustic resonance $\nu_{res} = 14.71$ MHz); *2* – for $\nu_s = 46.04$ MHz.
Arrows show the maxima positions calculated by Eq.(6c).

5. CONCLUSION

In the perfect silicon, US amplitude dependent pendulous beats of neutron diffraction intensity were observed. The oscillations are more pronounced in the case of neutron-acoustic resonance. The obtained experimental results mainly coincide with the theory.

In a low-deformed (bent) silicon single crystal a new type of "deformation pendellősung" has been revealed, with a period depending on the deformation gradient. Observation of such pendulous beats is linked to the use of high-frequency ultrasound and should be provided with at least several conditions: $B < 1$, $BT >> 1$ and $k_s/\Delta K_0 > 1$. These conditions are difficult to realise simultaneously in X-ray experiments.

Obviously, to observe the mentioned interference effects, some other methods could be used – e.g. the method consisting in direct observations of variations in spatial distribution of neutrons affected by ultrasound (the so-called "Kato's profiles") [16].

REFERENCES

1. Köhler, R., Möhling, W., & Peibst, H. (1974). *Phys. Status Solidi (b)* **61**, 439.
2. Mikula, P., Lukas, P., & Kulda J. (1992). *Acta Cryst. A.* **48**, 72.
3. Chukhovskii, F.N., Nosik, V.L., & Iolin, E.M. (1993). *Zh. Eksp. Teor. Fiz.* **104**, 2452.
4. Felber, J., Gähler, R., Rauch, C., & Golub, R. (1996). *Phys. Rev. A* **53** 1 319.
5. Aksenov, V., Gavrilov,V., Nikitenko,Yu., Progliado,V., & Raitman E. (2004). *Latv. J. Phys. Tech. Sci.* (3), 55.
6. Roshchupkin, D., Irzhak, D., Tucoulou, R., & Buzanov, O. (2003). *J. Appl. Phys.* **94**, (10), 6692.
7. Iolin, E., Farago, B., Raitman, E., & Mezei, F. (1998). *Physica B* **241-243** 1213.
8. Gavrilovs, V., Mjasishchevs, D., & Raitmans, E. (2005). *Latv. J. Phys. Tech. Sci.*, (1), 3.

9. Iolin, E., Zolotoyabko, E., Raitman, E. & Kuvaldin., B. (1986). *Zh. Eksp. Teor. Fiz.* **91**, 2132.
10. Iolin, E., Raitman, E., Kuvaldin, B., Gavrilov, V. & Zolotoyabko, E. (1988). *Zh. Eksp. Teor. Fiz.* **94**, 218.
11. Assur, K. & Entin, I. (1982). *Fiz. Tverd. Tela* **26**, 2122.
12. Kuvaldin, B. Theses. (1989). Ph. D. dissertation, Riga
13. Penning, P. (1966). *Philips Res. Rep.,* suppl., **5**, 1; Kato, N. (1964) *J. Phys. Soc. Jpn.* **19,** 67.
14. Iolin, E., Raitman, E., Gavrilov, V,. & Rusevich, L. (1995). *J. Phys. D.: Appl. Phys*. 28, A281.
15. Zolotoyabko, E. (1999). *Nucl. Instr. Methods,* **B131**, 410.
16. *Акустические кристаллы*. Справочник. (1982), М.: Наука.
17. Schull, C.C. (1973). *J. Appl. Cryst*., p.257-266

NEITRONU LAUES DIFRAKCIJA IDEĀLOS UN DEFORMĒTOS SILĪCIJA MONOKRISTĀLOS PIE ULTRASKAŅAS IEROSMES

E. Raitmans, V.Gavrilovs, M. Brezgunovs

K o p s a v i l k u m s

Izpētīta ultraskaņas ietekme uz neitronu Laues difrakciju ideālos un deformētos silīcija monokristālos. Ideālā kristālā novērotas difrakcijas relatīvās intensitātes oscilācijas, kas ir atkarīgas no ultraskaņas viļņu amplitūdas. Deformētā kristālā ultraskaņa izjauc parādīto punktu adiabātisko kustību pa dispersās virsmas plāksnēm. Tā rezultātā difrakcijas intensitāte krasi atšķiras no difrakcijas intensitātes ideālā kristālā. Iegūtie rezultāti labi saskan ar teorētisko koncepciju. Šie efekti var tikt izmantoti jaunu tipu neitronu monohromatoru un pārtraucēju radīšanā, kas vadāmi ar ultraskaņu

08.08.2008.